American Mineralogist, Volume 72, pages 756–765, 1987

Neutron and X-ray diffraction study of hydrogarnet $Ca_3Al_2(O_4H_4)_3$

G. A. Lager
Department of Geology, University of Louisville, Louisville, Kentucky 40292, U.S.A.
Th. Armbruster
Laboratory for Chemical and Mineralogical Crystallography, University of Bern, Freiestrasse 3, CH-3012, Bern, Switzerland,
J. Faber
Material Science and Technology Division, Argonne National Laboratory, Argonne, Illinois 60439, U.S.A.

Abstract

The crystal structure of $Ca_3Al_2(O_4D_4)_3$ was refined from time-of-flight neutron powder data collected at 300, 200, and 100 K. The D atom is located 0.906(1) Å (300 K) from oxygens surrounding the vacant $\bar{4}$ tetrahedral site. With the complete replacement of Si^{4+} by $4H^+$ in the grossular structure, the tetrahedral *d*–O distance increases from 1.645 to 1.950 Å. Structural adjustments in response to tetrahedral expansion include a decrease in the length of the shared octahedral edge relative to the unshared edge and a corresponding increase in the Ca(1)–O(4) distance in the dodecahedron. At low temperatures, the D tetrahedron rotates ~1° about the $\bar{4}$ axis relative to the rigid oxygen tetrahedron and becomes slightly more regular. The O–D distances at 300 and 100 K are within one standard deviation. Single-crystal X-ray intensity data were also obtained at 300 K from the same sample used in the neutron-diffraction experiments. The short O–H distance (0.65 Å) determined from the X-ray data is characteristic of mineral structures with non-H-bonded OH groups and OH groups with weak O–H···O interactions.

Introduction

The compound $Ca_3Al_2(O_4H_4)_3$ is the Si-free end member of the hydrogrossular series. Its structure was examined by Weiss et al. (1964) using X-ray powder methods and by Cohen-Addad et al. (1967) using neutron powder diffraction and NMR techniques. They concluded that $Ca_3Al_2(O_4H_4)_3$ was isostructural with grossular in space group *Ia*3*d* and that the hydrogarnet structure results from the replacement of $(SiO_4)^{4-}$ by $(OH)_4^-$. It was suggested that H substitutes for Si in such a way that each oxygen around the tetrahedral void is bonded to one H (O–H distance ~0.95 Å). The H has no additional oxygen neighbor within a 2.5-Å radius; thus it was classified as a "free" OH group without H bonds. A neutron powder refinement of a deuterated sample (Foreman, 1968) confirmed the existence of $(OD)_4^-$ as a structural entity. Bartl (1969) subsequently reported a single-crystal X-ray refinement, but no information on the H position was given.

The powder studies by Cohen-Addad et al. (1967) and Foreman (1968) were completed prior to the introduction of the Rietveld (1967) refinement procedure. The powder data were reduced in a manner analogous to single-crystal data, i.e., individual peaks were integrated to yield structure factors. As a result, only a few data were usable in these refinements (because of peak overlap), and these were in the high *d* range so that a certain amount of accuracy in the atomic parameters was lost. In the Rietveld method, the entire diffraction profile is fit point by point (e.g., at each 2θ step or time channel depending on whether a constant- or variable-wavelength source is used), and then the contribution of each Bragg reflection to the profile is determined. In addition to the limitations associated with the method of analysis, the accuracy of the above experiments may have been reduced by several other factors: (1) the sample used by Cohen-Addad et al. (1967) was not deuterated, i.e., the spin incoherent scattering from H would make a large contribution to background, effectively reducing signal-to-noise ratio and (2) the D position determined by Foreman was based on only nine neutron-diffraction reflections.

The present study reports neutron powder refinements of synthetic $Ca_3Al_2(O_4D_4)_3$ at 300, 200, and 100 K. The low-temperature refinements were included as part of the study for two reasons: (1) Reduced thermal vibrations at low temperatures should localize the D position and permit a more accurate determination of its position. (2) Renewed interest among mineralogists and petrologists in this mineral group has stemmed from the fact that hydrogarnets are potential storage sites for water in the Earth's mantle (Aines and Rossman, 1984). The temperature dependence of the $Ca_3Al_2(O_4D_4)_3$ structure could provide important information on the stability of naturally occurring hydrogarnets.

A single-crystal X-ray refinement at 300 K was also carried out to examine differences between the structures determined by X-ray and neutron diffraction (e.g., the

0003–004X/87/0708–0756$02.00

TABLE 2. Unit-cell and positional parameters and agreement factors (R) for neutron and X-ray refinements of $Ca_3Al_2(O_4H_4)_3$

		100 K	200 K	300 K	300 K (X-ray 1) (with H)	300 K (X-ray 2) (without H)
	a	12.5389(1)	12.5530(1)	12.5695(1)	12.565(3)	12.565(3)
O	x	0.0284(1)	0.0284(1)	0.0288(2)	0.02797(6)	0.0286(1)
	y	0.0525(1)	0.0523(1)	0.0522(1)	0.05260(5)	0.0528(1)
	z	0.6401(1)	0.6399(1)	0.6402(1)	0.63958(5)	0.6398(1)
D (H)	x	0.1521(1)	0.1523(1)	0.1517(1)	0.1723(11)	
	y	0.0899(1)	0.0904(1)	0.0913(1)	0.0931(11)	
	z	0.7995(1)	0.7986(2)	0.7985(2)	0.7989(11)	
	R_e = expected R	1.38	1.34	1.61		
	R_p = profile R	2.23	2.11	2.05		
	R_{wp} = weighted profile R	3.09	2.95	3.01		
	(R_w = weighted R, X-ray)				1.32	3.69
	R = unweighted R, X-ray				0.96	2.07
	R_R = Reitveld R	6.90	7.38	13.66		

Note: Numbers in parentheses are esds and refer to the last decimal place. All R values are expressed as percentages.

$R_e = f^{1/2}/(\Sigma_i w_i Y_{i,obs}^2)$

$R_p = (\Sigma_i | Y_{i,obs} - Y_{i,calc} |)/(\Sigma_i | Y_{i,obs} |)$

$R_{wp} = \{[\Sigma_i w_i (Y_{i,obs} - Y_{i,calc})^2]/(\Sigma_i w_i Y_{i,obs}^2)\}^{1/2}$

$R_w = \{[\Sigma_i w_i (F_{obs} - F_{calc})^2]/(\Sigma_i w_i F_{obs}^2)\}^{1/2}$

$R = (\Sigma | F_{obs} - F_{calc} |)/(\Sigma F_{obs})$

$R_R = (\Sigma_i | Y_{i,obs} - Y_{i,calc} |)/(\Sigma_i | Y_{i,obs} - B_i |)$,

where f is the number of degrees of freedom in the refinement, $Y_{i,obs}$, $Y_{i,calc}$, and B_i are the observed and calculated intensity and the background at the ith time channel, w_i is the weight, and F_{obs} and F_{calc} are the observed and calculated structure factors.

non-H-bonded OH group) and as a point of comparison with recent X-ray refinements of katoite $Ca_3Al_2(SiO_4)_{0.64}(O_4H_4)_{2.36}$ (Sacerdoti and Passaglia, 1985) and plazolite $Ca_3Al_2(SiO_4)_{1.53}(O_4H_4)_{1.47}$ (Basso et al., 1983), two members of the hydrogrossular series. These authors have reported different H positions that cannot be rationalized in terms of the hydrogarnet defect structure.

EXPERIMENTAL METHOD

A major problem in the preparation of $Ca_3Al_2(O_4D_4)_3$ involved the synthesis of tricalcium aluminate ($Ca_3Al_2O_6$), which reacts with D_2O at 473 K to form $Ca_3Al_2(O_4D_4)_3$. Initial attempts produced $Ca_3Al_2O_6$ together with $Ca_{12}Al_{14}O_{32}(OH)_2$. Even if very small amounts of $Ca_{12}Al_{14}O_{32}(OH)_2$ are present in the charge, it is impossible to obtain pure $Ca_3Al_2(O_4D_4)_3$ following hydrothermal treatment. In addition, since $Ca_{12}Al_{14}O_{32}(OH)_2$ contains hydroxyl groups, fully deuterated hydrogarnet cannot be prepared if this impurity is present. A pure sample of $Ca_3Al_2O_6$ was finally synthesized from a mixture of $CaCO_3$ and Al_2O_3 held at 1623 K for approximately one month. During the synthesis, the sample was reground at regular intervals (4 d) and then pressed into discs before reheating. Following each of the homogenization cycles, high-resolution Guinier X-ray photographs (λ = 1.9359 Å) were recorded to check for additional phases. Normally CaO was present in excess (in order to avoid formation of $Ca_{12}Al_{14}O_{32}(OH)_2$; see Figure 1 from Nurse et al., 1965) so that a small amount of Al_2O_3 had to be added at each stage until a pure product was obtained. The final product showed only one very weak CaO reflection after a 15-h exposure. The $Ca_3Al_2(O_4D_4)_3$ powder (~5 cm³) used in the neutron-diffraction experiments was prepared from $Ca_3Al_2O_6$ treated at 473 K and P_{D_2O} = 200 bars for a period of 8 d.

Time-of-flight neutron-diffraction data were collected at 300, 200, and 100 K for $Ca_3Al_2(O_4D_4)_3$ on the general-purpose powder diffractometer (GPPD) at the IPNS facility at Argonne National Laboratory. The data (Table 1)[1] were refined using a Rietveld (1967) profile analysis modified for spallation pulsed neutron sources (von Dreele et al., 1982). The D position was determined from difference Fourier analysis of the 100-K data. After refinement of positional parameters and anisotropic-temperature-factor coefficients for the non-D atoms [R_{wp} = 16.97%], a ΔF map revealed the D position at $x \approx 0.15$, $y \approx 0.09$, $z \approx 0.80$. Residual neutron density (~30% of D atom) was also observed at the oxygen position. The magnitude of the oxygen residual is not unusual for Rietveld analyses of pulsed neutron data (e.g., Rotella et al., 1982) and is probably due to systematic errors in fitting background or measuring the incident neutron spectrum. Inclusion of the D position in the least-squares refinement together with anisotropic-temperature-factor coefficients reduced the agreement factor to R_{wp} = 3.09% and produced an essentially featureless ΔF map (the largest peak was ~5% of an O atom). Refinement of the H/D site population indicated the presence of ~5% H (0.5 H per formula unit). The refinement model at each temperature included 621 allowed reflections in the d range 0.530–2.269 Å and 25 variable parameters, two of which defined the functional dependence of the background. Final agreement factors together with atom positional parameters are reported in Table 2. Anisotropic-temperature-factor coefficients are given in Table 3. The final refinement profile at 100 K is shown in Figure 1.

An equant dodecahedron (~125 μm in diameter) was picked from the same powder used in the neutron-diffraction experiment. After verifying space-group assignment with the precession method, the crystal was transferred to an ENRAF NONIUS CAD4 diffractometer (graphite-monochromated MoK_α radiation) for intensity measurements. The unit-cell parameter was deter-

[1] To obtain copies of Tables 1 and 4, order Document AM-87-344 from the Business Office, Mineralogical Society of America, 1625 I Street, N.W., Suite 414, Washington, D.C. 20006, U.S.A. Please remit $5.00 in advance for the microfiche.

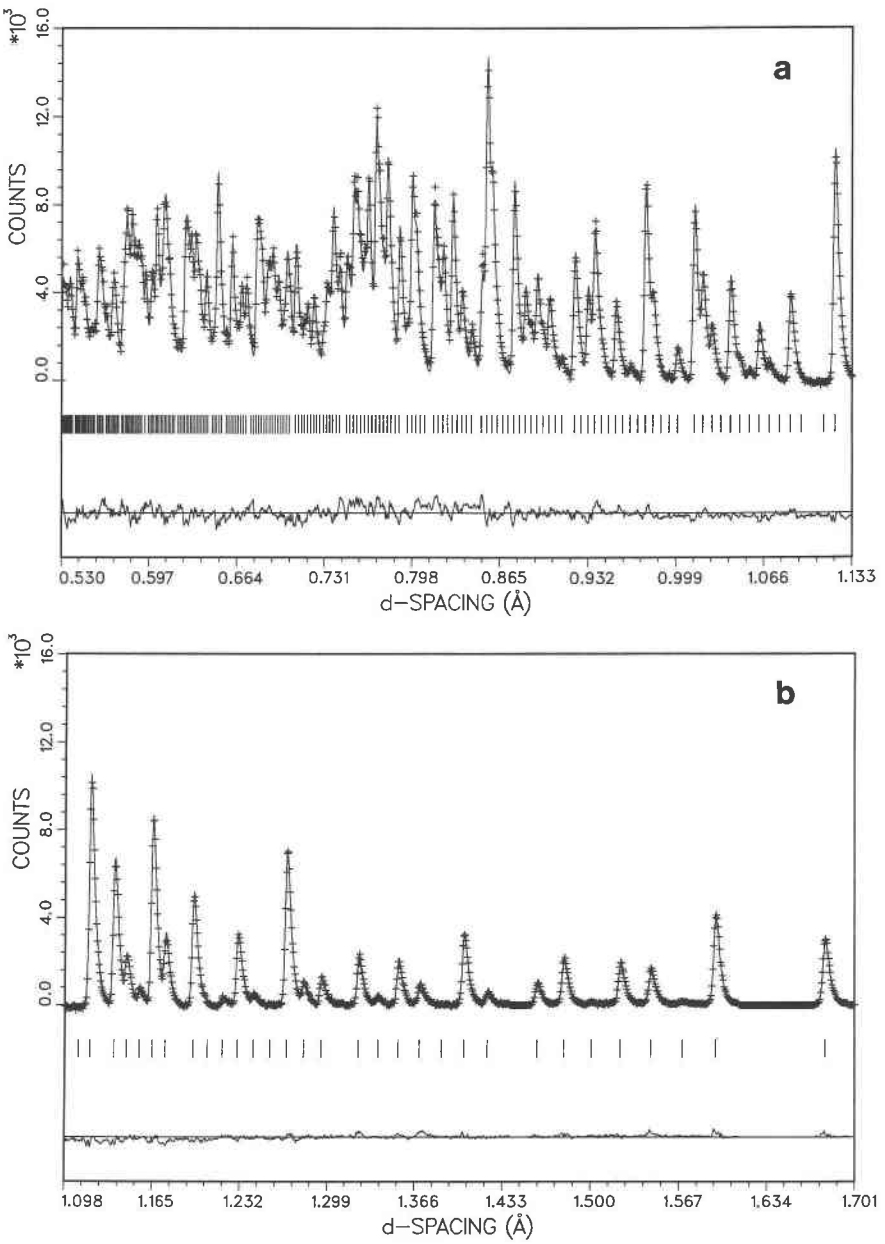

Fig. 1. Rietveld refinement profile for $Ca_3Al_2(O_4D_4)_3$ at 100 K (160° detectors). Plus marks are the raw data. Solid line is the best-fit profile. Tick marks below the profile indicate the positions of all allowed reflections. A difference curve (observed minus calculated) appears at the bottom. Background was fit as part of the refinement but has been subtracted before plotting.

mined from least-squares refinement of 25 automatically centered reflections ($25° > \theta > 10°$). Intensity data for all reflections (except those systematically absent from the I-centering operation) in one octant of the reciprocal space [$\theta_{max} = 30°$] were measured in an ω scan mode. Three standard reflections, measured in 5-h intervals to monitor X-ray intensity, showed a maximum variation of 3% throughout data collection. Data reduction, including background and Lorentz-polarization corrections, and least-squares refinements were carried out with the SDP (Enraf Nonius, 1983) program library. Intensity measurements (2329) were averaged to 327 unique observations, yielding an agreement factor on intensity of 2.3%. No absorption correction was applied because of crystal shape. Reflections (142) with $F_{obs} < 6\sigma F_{obs}$ were flagged as weak.

Structure-factor amplitudes (185) were weighted on the basis of counting statistics (Table 4; see footnote one). Neutral-atom scattering factors as supplied by the program were used. Excluding H, the refinement converged to $R = 2.07\%$, $R_w = 3.69\%$ with anisotropic-temperature-factor coefficients and a correction for secondary extinction (Tables 2 and 3). A difference Fourier section was then computed to determine the H position. Electron density, ellipsoidal in shape (0.4 e Å^{-3}) and initially attributed

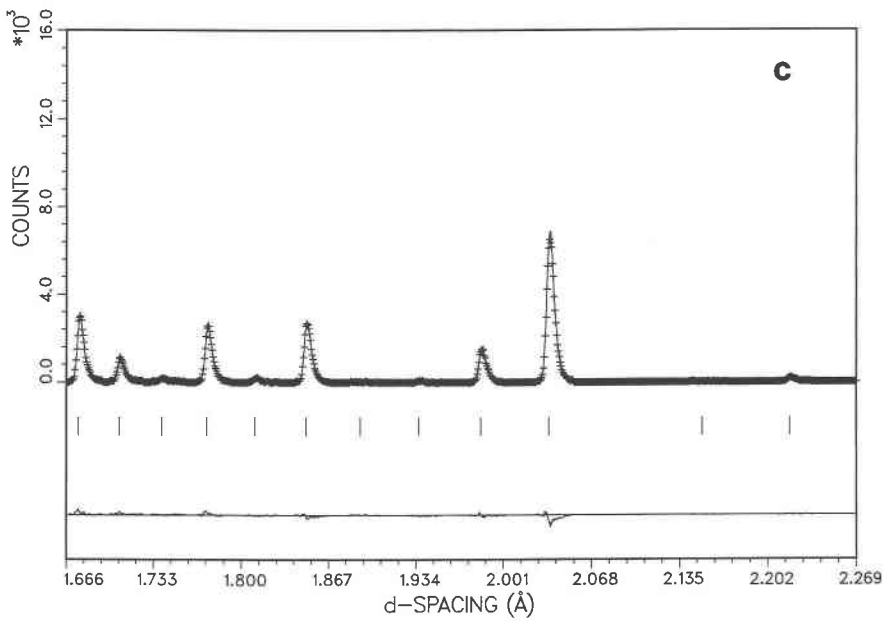

Fig. 1—*Continued.*

to H, was located ~0.7 Å from oxygen (background noise in the ΔF map was ~0.05 e Å^{-3}). Positional parameters derived from the ΔF map and an isotropic thermal parameter for H were varied in the following cycles of refinement (R = 1.05%, R_w = 1.45%). The electron density near the oxygen position (assumed H position) was so well defined that an anisotropic-temperature-factor refinement for H was attempted (R = 0.96%, R_w = 1.32%). Structural information relating to the X-ray refinements is included in Tables 2 and 3.

To verify the unusual H position (short O–H distance) obtained from the X-ray refinement, intensity data were collected for a second crystal picked from the same sample (212 unique reflections). All refined positional and anisotropic thermal parameters were identical within 1 esd for both crystals.

Results

The hydrogrossular defect structure can be represented in terms of the formula $^{VIII}Ca_3{}^{VI}Al_2(^{IV}SiO_4)_{3-x}(O_4H_4)_x$ where $x = 0$ refers to anhydrous grossular garnet and $x = 3$ the silica-free hydrogarnet end member. Superscripts in roman numerals refer to the three different types of cation

TABLE 3. Anisotropic-temperature-factor coefficients for neutron and X-ray refinements of $Ca_3Al_2(O_4H_4)_3$

		β_{11}	β_{22}	β_{33}	β_{12}	β_{13}	β_{23}
100 K	O	82(4)	121(5)	84(4)	−10(3)	−23(3)	−24(3)
	D	211(8)	497(11)	820(14)	−196(6)	−175(7)	262(8)
	Ca	134(12)	88(6)	88	0	0	−1(6)
	Al	50(5)	50	50	−13(6)	−13	−13
200 K	O	105(5)	144(5)	107(5)	−8(3)	−19(3)	−20(3)
	D	222(9)	519(2)	890(15)	−215(6)	−149(7)	235(9)
	Ca	142(2)	117(6)	117	0	0	1(7)
	Al	74(6)	74	74	−16(7)	−16	−16
300 K	O	197(8)	183(9)	120(8)	−19(6)	−4(5)	−63(5)
	D	293(5)	635(9)	1098(24)	−268(10)	−165(11)	249(13)
	Ca	172(9)	149(10)	149	0	0	−29(10)
	Al	94(10)	94	94	−80(10)	−80	−80
300 K (with H)	O	166(3)	193(3)	139(3)	−25(6)	−42(6)	−37(6)
	H*	3.3(3)					
	H	522(103)	421(104)	717(109)	355(154)	413(211)	490(201)
	Ca	169(2)	115(1)	114	0	0	23(3)
	Al	103(2)	103	103	−16(3)	−16	−16
300 K (without H)	O	185(9)	181(9)	129(9)	−30(16)	−12(16)	−45(16)
	Ca	171(4)	114(3)	114	0	0	32(8)
	Al	106(4)	106	106	−8(9)	−8	−8

Note: Values reported are $\times 10^5$. The coefficients are of the form $(\beta_{11}h^2 + \cdots + 2\,\beta_{12}hk + \cdots)$.
* Isotropic temperature factor.

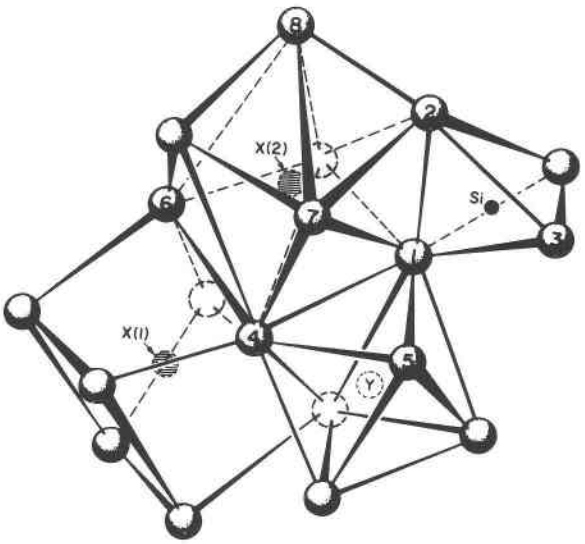

Fig. 2. A portion of the garnet structure showing the three different polyhedra and the numbering scheme for the atoms (Novak and Gibbs, 1971). In the grossular series, X(1) and X(2) refer to Ca^{2+} and Y represents Al^{3+}.

environments in the structure: the eight-coordinated triangular dodecahedral site, the six-coordinated octahedral site, and the tetrahedral site (Fig. 2). As indicated by the formula, H is incorporated in the structure via the isomorphic substitution $(OH)_4^- \rightleftharpoons (SiO_4)^{4-}$. This results in an expansion of the tetrahedra and a corresponding increase in the unit-cell parameter (Cohen-Addad et al., 1967). Interatomic distances and angles from this study are compared with previous work in Table 5. Although there are significant differences among the studies, the structure originally proposed by Cohen-Addad et al. (1967) is confirmed.

Oxygen and D tetrahedra

Figures 3a and 3b, based on the neutron powder refinements at 100 and 300 K, illustrate the atomic environment around the $\bar{4}$ site (*d* position). D atoms are located slightly above the face of the oxygen tetrahedron at a distance of 0.906 Å from oxygen. This distance is short compared to previous studies (Table 5) and short compared to other O–D distances determined by neutron-diffraction methods, where a mean value of 0.969(1) Å

TABLE 5. Comparison of interatomic distances and angles for $Ca_3Al_2(O_4H_4)_3$ studies

	1	2	3	4	5	6
			Tetrahedron			
d–O*	1.97(2)	1.924(2)	1.948(4)	1.950(2)	1.962(1)	1.956(2)
2 O(1)–O(2)	3.16(2)	3.022(6)	3.066(5)	3.058(2)	3.076(1)	3.070(3)
4 O(1)–O(3)	3.26(2)	3.200(6)	3.237(5)	3.245(2)	3.267(1)	3.255(2)
Mean	3.23	3.140	3.180	3.183	3.203	3.193
2 O(1)–Si–O(2)	105.6(6)	103.5(1)	103.8(1)	103.3(2)	103.19(4)	103.40(8)
4 O(1)–Si–O(3)	111.4(6)	112.5(1)	112.4(1)	112.7(2)	112.70(3)	112.59(7)
			Octahedron			
Al–O	1.89(2)	1.963(4)	1.920(4)	1.916(2)	1.906(1)	1.911(2)
6 O(1)–O(4)	2.57(2)	2.669(6)	2.612(5)	2.604(2)	2.578(1)	2.590(3)
6 O(1)–O(5)	2.77(2)	2.878(6)	2.813(5)	2.811(2)	2.810(1)	2.811(3)
Mean	2.67	2.774	2.713	2.708	2.695	2.701
6 O(1)–Al–O(4)	85.8(6)	85.6(1)	85.8(1)	85.6(2)	85.80(3)	85.31(6)
6 O(1)–Al–O(5)	94.2(6)	94.3(1)	94.3(1)	94.4(2)	94.92(3)	94.69(6)
			Dodecahedron			
4 Ca(1)–O(4)	2.50(2)	2.469(4)	2.474(4)	2.464(2)	2.462(1)	2.465(2)
4 Ca(2)–O(4)	2.50(2)	2.496(5)	2.514(4)	2.521(2)	2.511(1)	2.511(1)
Mean	2.51	2.483	2.494	2.493	2.487	2.488
2 O(1)–O(2)	3.15(2)	3.022(6)	3.066(5)	3.058(2)	3.076(1)	3.070(3)
4 O(1)–O(4)	2.57(2)	2.669(6)	2.612(5)	2.604(2)	2.578(1)	2.590(3)
4 O(1)–O(7)	3.77(2)	3.714(6)	3.739(5)	3.736(2)	3.738(1)	3.736(2)
4 O(4)–O(6)	3.11(2)	3.015(6)	3.072(5)	3.071(2)	3.059(1)	3.060(3)
2 O(4)–O(7)	2.97(2)	2.969(6)	3.007(5)	3.030(2)	3.031(1)	3.020(2)
2 O(7)–O(8)	4.03(2)	4.038(6)	4.048(5)	4.048(2)	4.023(1)	4.027(2)
Mean	3.23	3.203	3.219	3.218	3.213	3.210
2 O(1)–Ca(2)–O(2)	77.9(5)	75.4(1)	76.6(1)	76.7(1)	77.33(1)	77.04(7)
4 O(1)–Ca(2)–O(4)	61.9(5)	65.0(1)	63.1(1)	62.9(1)	62.45(2)	62.74(7)
4 O(1)–Ca(2)–O(7)	97.7(5)	96.8(1)	97.1(1)	97.1(1)	97.46(2)	97.33(6)
4 O(4)–Ca(2)–O(6)	76.8(5)	74.7(1)	76.0(1)	76.0(1)	75.91(2)	75.91(6)
2 O(4)–Ca(2)–O(7)	72.9(5)	73.0(1)	73.5(1)	73.9(1)	74.27(2)	73.97(4)
2 O(7)–Ca(2)–O(8)	107.6(5)	107.9(1)	107.2(1)	106.8(1)	106.36(2)	106.98(5)
O–H	0.95(3)	0.94(1)		0.904(2)	0.65(1)	
d–H	1.30(3)	1.24(1)		1.335(2)	1.43(1)	
Al–H	2.48(3)	2.47(1)		2.426(2)	2.29(1)	
Ca(1)–H	3.11(3)	3.08(1)		3.088(2)	2.86(1)	
Ca(2)–H	2.87(3)	2.94(1)		2.855(2)	2.75(1)	

Note: Columns are 1, Cohen-Addad et al. (1967); 2, Foreman (1968); 3, Bartl (1969); 4, present study, neutron powder refinement; 5, present study, single-crystal X-ray refinement with H; 6, present study, single-crystal X-ray refinement without H.

* *d* is Wyckoff notation for site with point symmetry $\bar{4}$ in space group *Ia*3*d* (occupied by Si in silicate garnets).

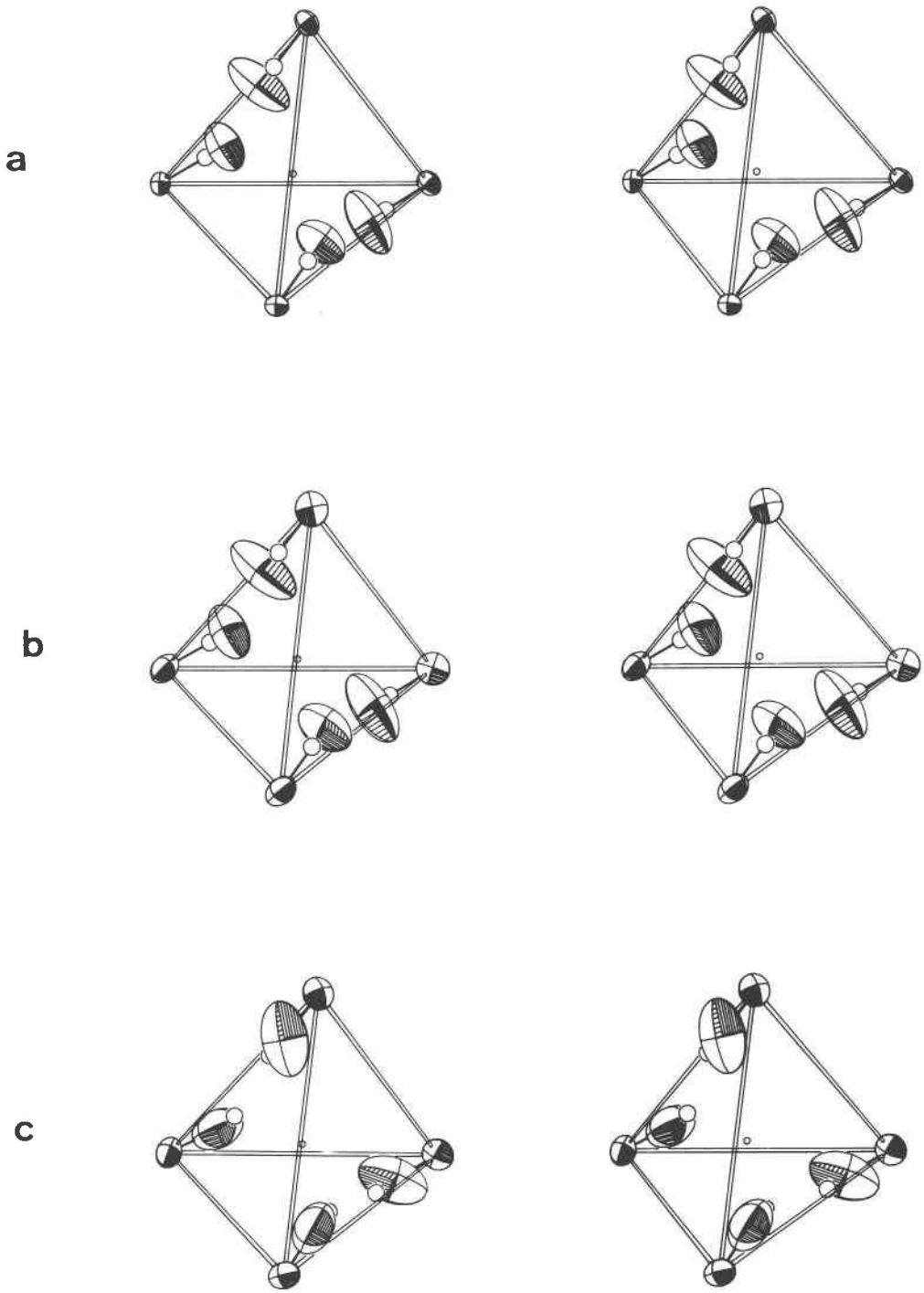

Fig. 3. Stereo ORTEP plots of atomic environment about the $\bar{4}$ site (*d* position) showing the oxygen tetrahedron with associated hydrogens (deuteriums). (a) Neutron refinement, 100 K; open circles along the O–D vector represent the position of displaced electrons as refined with X-rays. (b) Neutron refinement, 300 K [open circles as in (a)]. (c) X-ray refinement, 300 K; open circles at the end of the O–H vector represent the D position as refined with neutrons.

was observed (Ceccarelli et al., 1981). Although the O–D distance has not been corrected for thermal displacements (librational effects), it should be noted that the O–D distances at 300 and 100 K are within one standard deviation (Table 6). The displacement ellipsoids of D (Figs. 3a and 3b), which are oriented perpendicular to the O–D bond, show only minor differences between 100 and 300 K. Thus, a small amount of static (structure-averaged) positional disorder of the D seems more likely than dynamic (time-averaged) disorder.

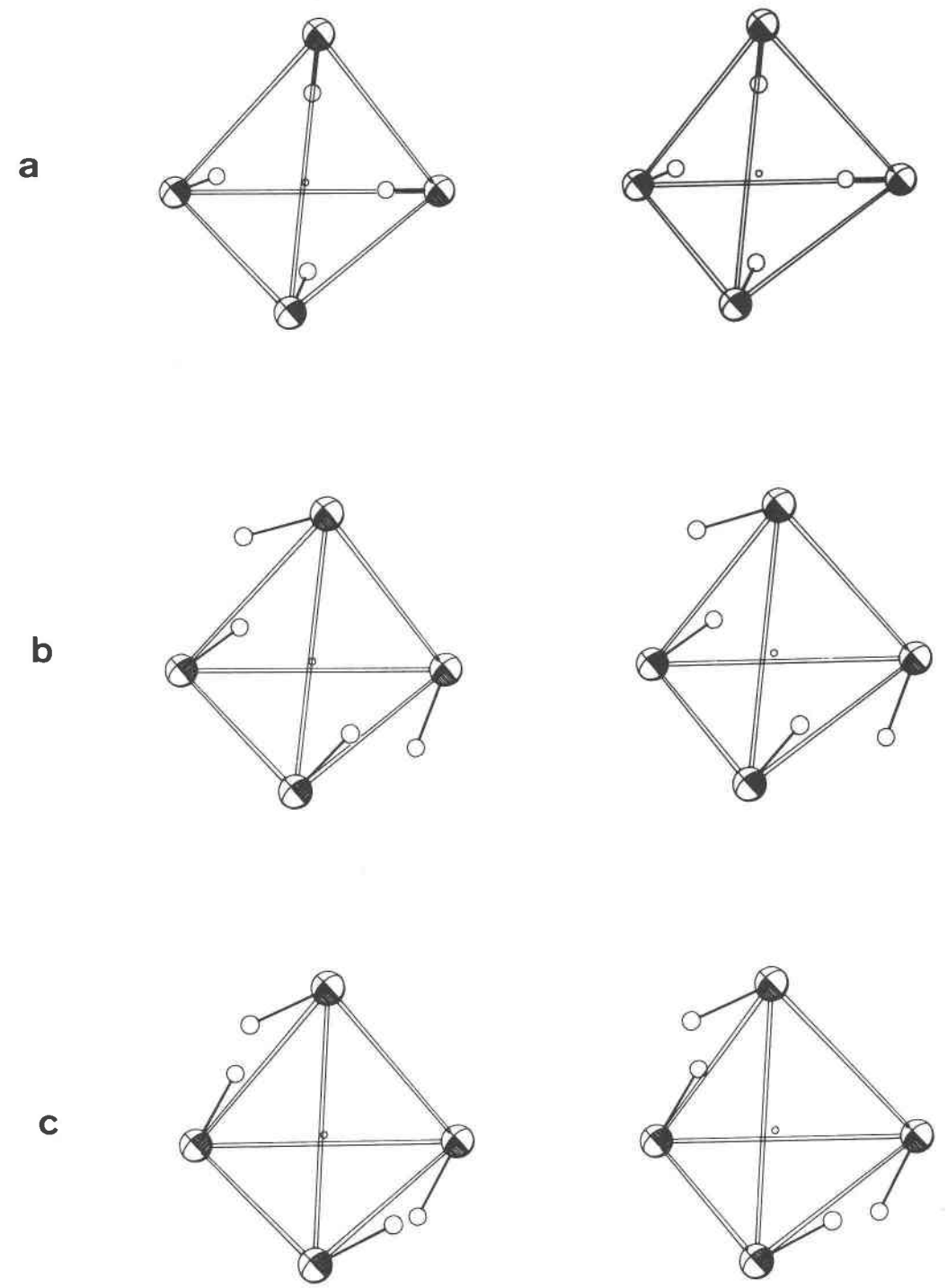

Fig. 4. Stereo ORTEP plots of atomic environment about the 4 site (*d* position) showing the oxygen tetrahedron with associated H positions. A constant diameter for oxygen and H spheres is used. (a) Katoite $Ca_3Al_2(SiO_4)_{0.64}(O_4H_4)_{2.36}$ (Sacerdoti and Passaglia, 1985). (b) Plazolite $Ca_3Al_2(SiO_4)_{1.53}(O_4H_4)_{1.47}$ (Basso et al., 1983). (c) Synthetic $Ca_3Al_2(SiO_4)_{2.16}(O_4H_4)_{0.84}$ (Cohen-Addad et al., 1967).

In most previous studies, O–D(H) distances were analyzed in compounds with rather strong O–D(H)···O H bonds that do not exist in hydrogarnets. Ceccarelli et al. (1981) and Ferraris and Franchini-Angela (1972) have observed that O–D distances determined by neutron diffraction become significantly shorter as the H bond D(H)···O becomes weaker (longer). Also, protons in OD(H) groups without additional oxygen neighbors, as in hydrogarnets, may not be rigidly bound. Therefore, static and/or dynamic disorder of the proton can be ex-

pected, which in turn can lead to an apparent shortening in the O–D(H) distance. Systematic studies of O–D(H) distances in isolated ("free") OD(H) groups have not been reported.

The O–H distance refined from X-ray data is only 0.65 Å (Fig. 3c). Although some shortening can be expected relative to the neutron determination, this value is anomalously short. However, the same results were obtained for both crystals investigated in this study, and comparable distances have also been reported for the Sr analogues of $Ca_3Al_2(O_4D_4)_3$ (0.78 Å—$Sr_3Al_2(O_4H_4)_3$; 0.68 Å—$Sr_3Fe_2(O_4H_4)_3$) (Nevskii et al., 1982). In vesuvianite, which has a structure closely related to garnet, Yoshiasa and Matsumoto (1986) reported a distance of only 0.6 Å for the non-H-bonded OH group (X-ray structure). In other structure types—e.g., datolite $CaBSiO_4(OH)$ (Foit et al., 1973), rosenhahnite $Ca_3Si_3O_8(OH)_2$ (Wan et al., 1977), and tinaksite $Ca_2K_2NaTi[Si_7O_{18}(OH)]$ (Bissert, 1980)—short O–H distances of ~0.75 Å have been observed for non-H-bonded OH groups (datolite) and OH groups with only weak O–H···O interactions (rosenhahnite, tinaksite). Therefore, we assume that for non-H-bonded OH groups, the residual density located near oxygen reflects the position of the displaced (bonding) electron between O and H and not the proton position. The orientation of the OH vector is very similar in the neutron and X-ray structures of $Ca_3Al_2(O_4H_4)_3$ (Fig. 3).

Sacerdoti and Passaglia (1985) have rationalized the short O–H distance of 0.68 Å in katoite $Ca_3Al_2(SiO_4)_{0.64}(O_4H_4)_{2.36}$ in terms of the hydrogarnet defect structure. When Si^{4+} occupies all tetrahedral sites (as in grossular), the *d*–O distance is 1.645 Å (Novak and Gibbs, 1971). In $Ca_3Al_2(O_4H_4)_3$ where all tetrahedral sites are vacant, the tetrahedra expand, and this distance lengthens to 1.950 Å (Table 5). The structure of katoite is intermediate: 80% of tetrahedral Si^{4+} is replaced by $4H^+$. The oxygen position refined from the X-ray data will therefore be an average position because two different oxygen sites can be occupied, i.e., one when Si^{4+} occupies the tetrahedral site, the other when this site is vacant. Sacerdoti and Passaglia (1985) have contended that the positional disorder associated with the oxygen atom obscures the H electron density and makes it very difficult to localize the H position with X-ray methods.

If the model proposed by Sacerdoti and Passaglia (1985) is correct, a similar result should have been obtained for plazolite, $Ca_3Al_2(SiO_4)_{1.53}(O_4H_4)_{1.47}$ (Basso et al., 1983). In both studies the H position was located by difference Fourier analysis and was not refined. However, Basso et al. (1983) reported a much longer O–H distance of 0.93 Å.

Figure 4 illustrates positions of the H atoms around the dO_4 tetrahedron (centered at $\bar{4}$) for katoite $Ca_3Al_2(SiO_4)_{0.64}(O_4H_4)_{2.36}$ (Sacerdoti and Passaglia, 1985), plazolite $Ca_3Al_2(SiO_4)_{1.53}(O_4H_4)_{1.47}$ (Basso et al., 1983) and synthetic $Ca_3Al_2(SiO_4)_{2.16}(O_4H_4)_{0.84}$ (Cohen-Addad et al., 1967). The OH vector in katoite points toward the center of the oxygen tetrahedron. The OH vectors in the other two members of the hydrogrossular series are located outside the tetrahedral faces as in $Ca_3Al_2(O_4D_4)_3$. Unfortunately, it is difficult to evaluate the accuracy of the H positions in the above structures. As mentioned previously, the H position in plazolite and katoite is based on difference Fourier analysis of X-ray diffraction data. The H position in synthetic hydrogrossular was determined from a protonated sample using a limited number of neutron powder data (20 reflections).

TABLE 6. Interatomic distances and angles for $Ca_3Al_2(O_4H_4)_3$ at three temperatures

	100 K	200 K	300 K
	Tetrahedron		
d–O*	1.948(1)	1.952(1)	1.950(2)
2 O(1)–O(2)	3.052(2)	3.060(2)	3.058(2)
4 O(1)–O(3)	3.244(2)	3.250(2)	3.245(2)
Mean	3.180	3.187	3.183
2 O(1)–Si–O(2)	103.1(1)	103.2(1)	103.3(2)
4 O(1)–Si–O(3)	112.7(1)	112.7(1)	112.7(2)
	Octahedron		
Al–O	1.911(1)	1.908(1)	1.916(2)
6 O(1)–O(4)	2.590(2)	2.588(2)	2.604(2)
6 O(1)–O(5)	2.809(2)	2.805(2)	2.811(2)
Mean	2.700	2.697	2.706
6 O(1)–Al–O(4)	85.4(1)	85.4(1)	85.6(2)
6 O(1)–Al–O(5)	94.7(1)	94.6(1)	94.4(2)
	Dodecahedron		
4 Ca(1)–O(4)	2.456(1)	2.460(1)	2.464(2)
4 Ca(2)–O(4)	2.509(1)	2.514(1)	2.521(2)
Mean	2.483	2.487	2.493
2 O(1)–O(2)	3.052(2)	3.060(2)	3.058(2)
4 O(1)–O(4)	2.590(2)	2.588(2)	2.604(2)
4 O(1)–O(7)	3.725(2)	3.731(2)	3.736(2)
4 O(4)–O(6)	3.052(2)	3.060(2)	3.071(2)
2 O(4)–O(7)	3.022(2)	3.029(2)	3.030(2)
2 O(7)–O(8)	4.024(2)	4.031(2)	4.048(2)
Mean	3.204	3.209	3.218
2 O(1)–Ca(2)–O(2)	76.9(1)	76.9(1)	76.7(1)
4 O(1)–Ca(2)–O(4)	62.9(1)	62.7(1)	62.9(1)
4 O(1)–Ca(2)–O(7)	97.2(1)	97.2(1)	97.1(1)
4 O(4)–Ca(2)–O(6)	75.9(1)	76.0(1)	76.0(1)
2 O(4)–Ca(2)–O(7)	74.1(1)	74.1(1)	73.9(1)
2 O(7)–Ca(2)–O(8)	106.6(1)	106.6(1)	106.8(1)
O–D	0.905(1)	0.905(1)	0.906(2)
d–D	1.331(1)	1.333(1)	1.343(2)
Al–D	2.433(1)	2.427(1)	2.425(2)
Ca(1)–D	3.075(1)	3.078(1)	3.094(2)
Ca(2)–D	2.831(1)	2.843(1)	2.851(2)

* *d* is Wyckoff notation for site with point symmetry $\bar{4}$ in space group *Ia3d*.

Oxygen positions determined by neutron and X-ray diffraction are significantly different (Table 2). If H is not considered in the X-ray refinement, this discrepancy becomes less pronounced. At this point, it is not understood whether these differences represent real effects, related to the electron polarization of oxygen, or whether the esds in the X-ray or neutron refinement are underestimated.

Al octahedron

Although the *d*–O distance in grossular (1.645 Å) lengthens to 1.950 Å with the complete replacement of Si^{4+} by $4H^+$, the Al–O distances in the two structures are

TABLE 7. Variation in octahedral distances and angles for four garnets in hydrogrossular series

	Grossular*	Plazolite†	Katoite‡	$Ca_3Al_2(O_4H_4)_3$§
Al–O	1.924(1)	1.927(1)	1.902(2)	1.916(2)
6 O(1)–O(4)	2.756(2)	2.701(2)	2.607(2)	2.604(2)
6 O(1)–O(5)	2.686(2)	2.750(2)	2.769(3)	2.811(2)
Mean	2.721	2.725	2.688	2.708
6 O(1)–Al–O(4)	91.5(1)	89.0(1)	86.6(1)	85.6(2)
6 O(1)–Al–O(5)	88.5(1)	91.0(1)	93.4(1)	94.4(2)

* Novak and Gibbs (1971).
† Basso et al. (1983).
‡ Sacerdoti and Passaglia (1985).
§ This study, neutron refinement.

very similar (1.924 vs. 1.916 Å). The major effect of the $(OH)_4^- \rightleftharpoons (SiO_4)^{4-}$ substitution is observed in the octahedral edges. In grossular, the shared edge (2.756 Å) is longer than the unshared edge (2.686 Å). An inverse relationship exists in $Ca_3Al_2(O_4H_4)_3$ (neutron refinement) where the shared edge (2.604 Å) is much shorter than the unshared edge (2.811 Å). The mean O–O edge actually decreases from 2.721 Å in grossular to 2.708 Å in $Ca_3Al_2(O_4H_4)_3$, i.e., the octahedron changes dramatically in shape but not size.

Table 7 compares octahedral distances and angles in grossular and $Ca_3Al_2(O_4H_4)_3$ with those in two other members of the hydrogrossular series, plazolite (Basso et al., 1983) and katoite (Sacerdoti and Passaglia, 1985). With increasing OH content in the series, the shared edge decreases in length whereas the unshared edge increases. These changes apparently reflect adjustments in the structure as the tetrahedral edge expands. The tetrahedra share two edges with triangular dodecahedra, which, in turn, share four edges with octahedra.

Sacerdoti and Passaglia (1985) have suggested a correlation between the degree of hydration in garnets and the relative lengths of the shared and unshared octahedral edges. Garnets, like grossular, could effectively incorporate large amounts of OH by decreasing the shared octahedral edge. If however, the shared edge is shorter than the unshared edge., e.g., as in pyrope, the degree of hydration possible would be much less because the length of the shared edge (2.618 Å) would soon approach the lower limit for an O–O distance. This line of reasoning is consistent with the occurrence of hydrogarnets in nature, i.e., garnets with substantiated high water contents (>1 wt% H_2O) also have high grossular and/or andradite components (Basso et al., 1984).

Because of their high *T-P* stability and occurrence in ultramafic rocks (e.g., peridotite and eclogite xenoliths) garnets are thought to be important constituents of the Earth's mantle. The degree of hydration in pyrope-rich garnets is an important question with regard to the availability of water at these depths. Assuming the proposal by Sacerdoti and Passaglia (1985) has some validity, the length of the shared octahedral edge at 300 K would seem to preclude the occurrence of water-rich pyropes at the Earth's surface. A knowledge of the relative lengths of the octahedral edges at mantle conditions requires information on the *T-P* dependence of the structure. Variations in the octahedral edges as a function of *T* (Meagher, 1975) and *P* (Hazen and Finger, 1978) show an inverse relationship in pyrope. The shared octahedral edge exhibits a greater thermal expansion and a larger compression relative to the unshared edge. One might speculate that the combined effect of *T* and *P* would be to produce only small changes in the lengths of the octahedral edges. In this case, the pyrope structure could only incorporate very limited amounts of water at mantle temperatures and pressures.

Triangular dodecahedron

The increase in the shared tetrahedral edge (and corresponding decrease in the shared octahedral edge) in $Ca_3Al_2(O_4H_4)_3$ relative to grossular results in a lengthening of the Ca(1)–O(4) distance from 2.319 (in grossular) to 2.464 Å (Fig. 2). By contrast, the Ca(2)–O(4) distance increases by only 0.03 Å. In anhydrous garnets, as the size of the dodecahedron increases, the shared octahedral edge increases relative to the unshared edge (Novak and Gibbs, 1971). A similar trend does not exist in the hydrogrossular series because the tetrahedron does not behave as a rigid structural element. In addition to an increase in size, the tetrahedron undergoes a rigid body rotation ($\gamma = 25.4°$)[2] about the $\bar{4}$ axis. Rotation to larger γ values relative to grossular ($\gamma = 24.5°$) lengthens the unshared octahedral edge and shortens the shared edge (Meagher, 1975, Fig. 6).

Temperature dependence of the $Ca_3Al_2(O_4H_4)_3$ structure

Only small structural changes occur in $Ca_3Al_2(O_4H_4)_3$ as the temperature is decreased from 300 to 100 K (Table 6). The oxygen tetrahedron remains essentially rigid with the possible exception of the shared edge O(1)–O(2). The D tetrahedron rotates ~1° about the $\bar{4}$ axis relative to the oxygen tetrahedron and becomes slightly more regular at lower temperature. Distances between D atoms are 2.599 and 1.956 Å at 300 K vs. 2.574 and 1.943 Å at 100 K. The O–D distance at 100 K is within one standard deviation of its value at room temperature. The major change in the structure occurs in the dodecahedron where the mean Ca–O distance decreases from 2.493 to 2.483 Å. Both the shared tetrahedral edge O(1)–O(2) and the shared octahedral edge O(1)–O(4) decrease at lower temperatures, in contrast to their inverse relationship in the hydrogrossular series.

ACKNOWLEDGMENTS

G.A.L. acknowledges support of this research by the National Science Foundation (Experimental and Theoretical Geochemistry) through Grant EAR-8205605. The neutron-scattering experiments were carried out at

[2] Meagher (1975) defined the positional angle γ as "the smaller of two angles between the tetrahedral O–O edge normal to the $\bar{4}$ axis and the two crystallographic axes normal to the $\bar{4}$-axis."

the Argonne Intense Pulsed Neutron Source. J.F. acknowledges support by USDOE, BES–Materials Science under contract W31-109-ENG-38.

REFERENCES

Aines, R.D., and Rossman, G.R. (1984) Water content of mantle garnets. Geology, 12, 720–723.

Bartl, H. (1969) Rontgen Einkristalluntersuchungen an $3CaO \cdot Al_2O_3 \cdot 6H_2O$ und an $12CaO \cdot 7Al_2O_3 \cdot H_2O$: Neuer Vorschlag zur 12 $CaO \cdot 7Al_2O_3$ Struktur. Neues Jahrbuch für Mineralogie Monatshefte, 404–413.

Basso, R., Della Giusta, A., and Zefiro, L. (1983) Crystal structure refinement of plazolite, a highly hydrated natural hydrogrossular. Neues Jahrbuch für Mineralogie Monatshefte, 251–258.

Basso, R., Cimmino, F., and Messiga, B. (1984) Crystal chemistry of hydrogarnets from three different microstructural sites of a basaltic metarodingite from Voltri massif (Western Liguria, Italy). Neues Jahrbuch für Mineralogie Abhandlungen, 148, 246–258.

Bissert, G. (1980) Verfeinerung der Struktur von Tinaksit, $Ca_2K_2NaTiO[Si_7O_{18}(OH)]$. Acta Crystallographica, B36, 259–263.

Ceccarelli, C., Jeffrey, G.A., and Taylor, R. (1981) A survey of O–H···O hydrogen bond geometries determined by neutron diffraction. Journal of Molecular Structure, 70, 255–271.

Cohen-Addad, C., Ducros, P., and Bertaut, E.F. (1967) Etude de la substitution du groupement SiO_4 par $(OH)_4$ dans les composés $Al_2Ca_3(OH)_{12}$ et $Al_2Ca_3(SiO_4)_{2.16}(OH)_{3.36}$ de type grenat. Acta Crystallographica, 23, 220–230.

Enraf-Nonius. (1983) Structure determination package (SDP). Enraf-Nonius, Delft.

Ferraris, G., and Franchini-Angela, M. (1972) Survey of the geometry and environment of water molecules in crystalline hydrates studied by neutron diffraction. Acta Crystallographica, B28, 3572–3583.

Foit, F.F., Jr., Phillips, M.W., and Gibbs, G.V. (1973) A refinement of the crystal structure of datolite, $CaBSiO_4(OH)$. American Mineralogist, 58, 909–914.

Foreman, D.W. (1968) Neutron and X-ray diffraction study of $Ca_3Al_2(O_4D_4)_3$, a garnetoid. Journal of Chemical Physics, 48, 3037–3041.

Hazen, R.M., and Finger, L.W. (1978) Crystal structures and compressibilities of pyrope and grossular to 60 kbar. American Mineralogist, 63, 297–303.

Meagher, E.P. (1975) The crystal structures of pyrope and grossularite at elevated temperatures. American Mineralogist, 60, 218–228.

Nevskii, N.N., Ivanov-Emin, B.N., and Nevskaya, N.A., Kaziev, G.Z., and Belov, N.V. (1982) Crystal structure of strontium hydrogarnets. Soviet Physics, Doklady 27, 427–428.

Novak, G.A., and Gibbs, G.V. (1971) The crystal chemistry of the silicate garnets. American Mineralogist, 56, 791–825.

Nurse, R.W., Welch, J.A., and Majumdar, A.J. (1965) The CaO-Al_2O_3 system in moisture-free atmosphere. British Ceramic Society Transactions, 64, 409–418.

Rietveld, H.M. (1967) Line profiles of neutron powder diffraction peaks for structure refinement. Acta Crystallographica, 22, 151–152.

Rotella, F.J., Jorgensen, J.D., Biefeld, R.M., and Morosin, B. (1982) Location of deuterium sites in defect pyrochlore $DTaWO_6$ from neutron powder diffraction data. Acta Crystallographica, 1338, 1697–1703.

Sacerdoti, M., and Passaglia, E. (1985) The crystal structure of katoite and implications within the hydrogrossular group of minerals. Bulletin de Minéralogie, 108, 1–8.

von Dreele, R.B., Jorgensen, J.D., and Windsor, C.G. (1982) Rietveld refinement with spallation neutron powder diffraction data. Journal of Applied Crystallography, 15, 581–589.

Wan, C., Ghose, S., and Gibbs, G.V. (1977) Rosenhahnite, $Ca_3Si_3O_8(OH)_2$: Crystal structure and the stereochemical configuration of the hydroxylated trisilicate group, $[Si_3O_8(OH)_2]$. American Mineralogist, 62, 503–512.

Weiss, R., Grandjean, D., and Palvin, J.L. (1964) Structure de l'aluminate tricalcique hydrate, $3CaO \cdot Al_2O_3 \cdot 6H_2O$. Acta Crystallographica, 17, 1329–1330.

Yoshiasa, A., and Matsumoto, T. (1986) The crystal structure of vesuvianite from Nakatatsu mine: Reinvestigation of the cation site-populations and of the hydroxyl groups. Mineralogical Journal, 13, 1–12.

MANUSCRIPT RECEIVED NOVEMBER 14, 1986
MANUSCRIPT ACCEPTED APRIL 24, 1987